The 4th European sCO_2 Conference for Energy Systems
March 23-24, 2021, Online Conference

2021-sCO2.eu-112

TECHNO-ECONOMIC OPTIMIZATION METHOD AND ITS APPLICATION TO AN SCO_2 GAS TURBINE BOTTOMING CYCLE

Thiago Gotelip*
Technische Universität Dresden
Dresden, Germany
Email: Thiago.Gotelip_Correa_Veloso@tu-dresden.de

Uwe Gampe
Technische Universität Dresden
Dresden, Germany

Stefan Glos
Siemens Energy AG
Mülheim, Germany

ABSTRACT

Cycle architecture, fluid parameter selection, and component design of an exhaust/waste heat recovery cycle require an integral approach. The exhaust/waste heat shall be utilized to a maximum but at minimum costs. The bottoming cycle needs to be aligned with the topping cycle regarding operational behavior, especially for a part load. To analyze potentials of exhaust heat recovery in a combined gas turbine sCO2 cycle, the bottoming cycle's optimum cycle architecture and fluid parameters must be determined. A thermo-physical model of the sCO2 bottoming cycle, including knowledge of component design, component behavior, and costs, is based on the multiobjective optimization procedure. As part of the CARBOSOLA project, techno-economic optimizations for a use case of exhaust heat recovery have been carried out. The paper aims to present the optimization methodology followed by the specific use case's boundary conditions, investigated sCO2 cycle architectures, and results of optimum cycle architecture and fluid parameters for maximum heat recovery and minimum costs. Attention will also be paid to accurate modeling of heat exchangers operating near the critical point.

INTRODUCTION

Over the last decade, the application of supercritical CO_2 (sCO_2) for power generation has received substantial interest as the technology prospects shows high efficiency, compact equipment, low emission, higher operational flexibility and lower plant complexity.

The sCO_2 cycle operation near the CO_2 critical point gives the cycle essential characteristics such as very compact turbomachines, a compression in an almost incompressible region, allowing good efficiency characteristics to the compressor. Thus, this technology combines the advantages of the steam Rankine cycle and gas turbine cycle.

The thermodynamic properties suffer significant variations near the critical point, and the determination of these characteristics in this region as heat transfer and pressure drop of carbon dioxide (CO_2) are difficult to predict. These are crucial issues for the design of the cycle. Wahl [1] propose an investigation of the heat transfer and pressure drop of carbon dioxide near the critical point cooled in a 2 mm diameter. Significant effects on the mass flux, inlet pressure and cooling temperature on the heat transfer was analyzed. The investigations in [2–4] also present the characteristics of the SCO_2 cycle near the pseudo-critical point.

Accurate thermo-economic analysis of sCO_2 cycles is a driver for the development of the technology. Weiland et al., [5] reports on sCO_2 component cost scaling relationships that have been developed collaboratively from an aggregate set of vendor quotes, cost estimates, and published literature. Thermo-economic evaluation of sCO_2 power cycle design is also investigated in [6–8].

Several sCO_2 cycle architecture have been analyzed in previous studies. Milani et al., [9] identified in their study 14 representations of sCO_2 cycles from the literature. The authors categorized these representations into three common features sub-groups depending on the expected enhancement effect in the cycle thermal efficiency calculation: (1) heat recuperation enhancement, (2) turbine work boosting, and (3) compression work reduction. Crespi et al., [10] presented in their study a systematic thermodynamic analysis of 12 supercritical carbon dioxide cycles under similar working conditions. The analysis regarding different architectures is also analyzed in [11,12].

Recent studies on sCO_2 cycle optimization are summarized in [13]. The authors compile several analyses and optimization of the sCO_2 power cycle from the different aspects, including different types of heat sources, high-efficiency heat exchangers, cycle layouts and optimizations, and aerodynamic design of turbomachinery. Optimizations regarding cycle performance and

* corresponding author(s)

DOI: 10.17185/duepublico/73953

economic analysis are the objectives of other investigations like [14,15].

The multiobjective optimization proposed in this study evaluates different conflicting objective functions. A parametric analysis is insufficient for a comprehensive evaluation of the systems' performance investigated.

The multiobjective optimization process is very susceptible to objective functions, cost models, economic evaluation boundaries, equipment design, and equipment efficiency. This analysis is essential to provide the optimal operation conditions since only the precise combination of these variables allows the best technical and economic performance.

CARBOSOLA PROJECT

The CARBOSOLA project presented in this paper is intended to represent the entry into sCO_2 technology development in Germany. This requires an analysis of the expected advantages. Therefore, the sCO_2 technology will be compared with conventional technologies in the fields of waste and exhaust heat recovery (bottoming cycles of combined cycle gas turbine plants) and solar-thermal power plant technology (CSP) and subjected to a technical-economic evaluation. The technology comparison is intended to show what increase in efficiency can be expected when using sCO_2 compared to water/steam and what the electricity production costs are. However, the core of the project is the component and system design of a technology demonstrator to use secondary heat, construction and commissioning of a test loop, and the methods required for further technology development up to commercial maturity.

The consortium of public funded project CARABOSOLA under the lead of Siemens Energy comprises of four partners. TU Dresden and the Helmholtz Zentrum Dresden-Rossendorf covering the necessary scientific-technical investigations for technology and product development. Furthermore, DLR provides the expertise for the evaluation of solar thermal power plants and Siemens Energy has a high level of expertise in the field of power plant technology and covers the necessary know-how of all components involved such as turbines, compressors and heat exchangers.

THERMODYNAMIC PERFORMANCE

In this first work package of CARBOSOLA the exhaust heat of two aeroderivative gas turbines was defined as use case for the optimization of a sCO_2 cycle. Those gas turbines are often applied for mechanical drive of compressors in the oil and gas industry. Another application is combined heat and power generation. The thermodynamic boundaries of the considered use case are listed in Table 1.

The conceptual design process consists of two major activities – selecting the cycle architecture and sizing the equipment. The term “cycle architecture” refers to the general arrangement of turbines, pumps, recuperators and external heat exchangers. [14]

In this study, the optimization of five different architectures will be evaluated. This methodology considered the analysis of less complex configurations such as the Simple and Regenerative cycle and more elaborate architectures, referenced as the number of their heat exchangers (heater and recuperator): 3H2R, 2H2R, 2H1R.

Table 1 Exhaust Gas Characteristics

Heat Source	2 x AGT on 1 sCO_2
Pressure [bar]	1,04
Temperature [°C]	432
Cold Flue Gas Temperature [°C]	≥ 75
Mass Flow [kg/s]	337
Wet cooling tower parameters:	
Ambient Temperature [°C]	15
Wet Bulb Temperature [°C]	10,8
Approach Temperature [°C]	5
Warm Up Range [°C]	7

The 3H2R architecture, Figure 1, is based on the Dual Rail cycle configuration proposed in [16]. This configuration performs source heat recovery using three heaters and a high-temperature recuperator and low-temperature recuperator. This architecture is also discussed in [14,17,18] for the heat recovery of gas turbines. The schematic representation of the other architectures is presented in the annex.

The 2H2R architecture is a reference to the cascade cycle, originally proposed [19]. This configuration is composed of two heaters and two recuperators. This architecture is also investigated in [20] and [21], with modifications, such as one more compressor with intercooling.

The 2H1R architecture was proposed to combine the less complex cycles' characteristics with the more elaborate arrangements. This one is composed of two heaters and only one recuperator, of high temperature.

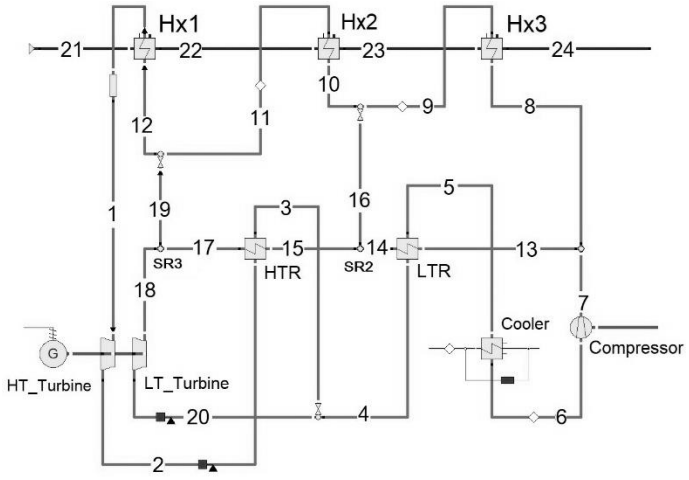

Figure 1: Layout scheme of sCO_2 architecture.

In Simple and Regenerative cycles, only one turbine performs the expansion, while the other configurations bases on processes divided into a high temperature and a low-temperature turbine. This study considers the split expansion as an optimization criterion in this study. In this way, the cycles' operation is also evaluated with the system's simplification using only one turbine. The consideration of this criterion modifies the

3H2R and 2H2R cycles of the same ones that were initially based.

Due to the variation of the CO_2 properties close to the critical point, the pinch point restriction is a fundamental constraint in sCO_2 operations. Figure 2 illustrates the behavior of the specific heat capacity for CO_2 using Refprop® data.

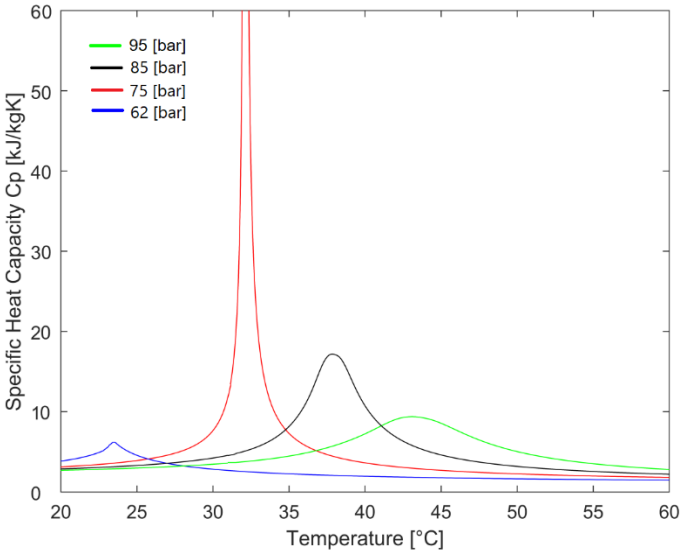

Figure 2: Specific heat capacity of CO_2 near the critical point. Elaborate by the author with Refprop® data.

As can be observed for each of the pressures in the supercritical region, above the critical CO_2 pressure, the specific heat capacity passes through a peak when it crosses the pseudocritical temperature. The pseudocritical temperature increases with the pressure, and moreover, the distinct peaks are flattened. [1]

The thermal conductivity to CO_2 in this region also shows a similar behavior, linked to the specific heat capacity behavior, Figure 3.

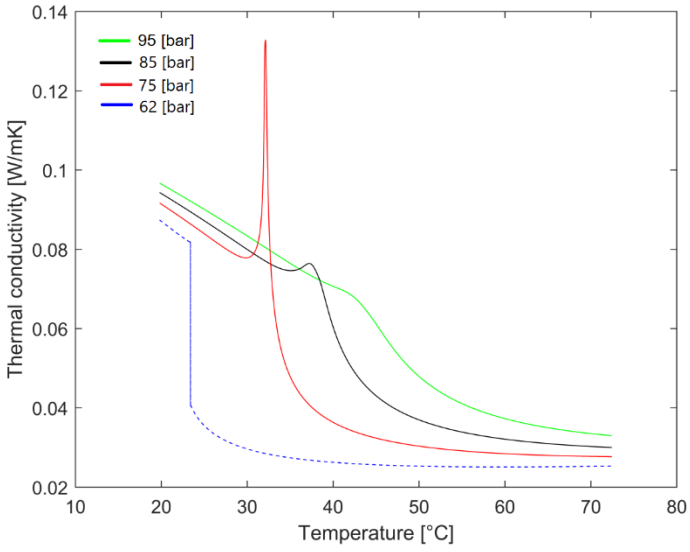

Figure 3: Thermal conductivity of CO_2 near the critical point. Elaborate by the author with Refprop® data.

In the gas region, the thermal conductivity increases when approaching the pseudocritical temperature. The higher pressures present higher thermal conductivity before the peak, although the value at the peak increases with the decreasing pressure. The pressure also shifts the pseudocritical temperature.

The properties of CO_2 close to the critical point is the object of study of [2–4]. The variation of these properties is a determining factor for the heat exchangers' design, significantly the cooler. The heat exchangers analysis in these cycles should be carefully investigated.

For calculating CO_2 properties in each heat exchanger, the variable property segmented calculation method (VPSC) is considered more suitable for non-constant thermal capacities process streams.

The VPSC method for property calculations consists of dividing the heat exchangers into several small blocks along the length. This methodology determines the working fluid's physical properties according to each block's inlet and outlet pressures, and the temperature is calculated by the LTMD method at each block. The overall conductance UA in each heat exchanger is defined by equations 1 and 2.

$$U \cdot A = \sum_{i=1}^{n} \left(\frac{\dot{Q}_i}{LMTD_i} \right) \quad (1)$$

$$LMTD = \left[\frac{(\Delta T_{hot} - \Delta T_{cold})}{ln(\Delta T_{hot} / \Delta T_{cold})} \right] \quad (2)$$

i= number of segments for the heat exchanger.

In conventional LMTD, physical property is assumed to be constant during the solving process. According to Ke et al. [22], the LMTD is not appropriate for the thermal design of heat exchanger for sCO_2 applications, and the VPSC can be used to obtain more reliable results. The optimization tool model considers each heat exchanger's analysis divided into 100 sections to avoid these analysis errors. The method validation with Ebsilon indicated relative errors lower than 0.1 The same methodology is adopted by Held [14] for a 25 sub-element discretized heat exchanger model.

ECONOMIC ANALYSIS

The equipment cost model follows the study of [5]. In this study, the authors used data from 93 vendor quotes to generate component cost models. The general equation for the cost of equipment is determined by [5]:

$$C = aSP^b \times f_T \quad (3)$$

Where C is the component cost, a and b are fit coefficients, SP is the scaling parameter, and f_T is a temperature correction factor described by [5]:

$$f_T = \begin{cases} 1 \; if \; T_{max} < T_{bp} \\ 1 + c(T_{max} - T_{bp}) + d(T_{max} - T_{bp})^2 \; if \; T_{max} \geq T_{bp} \end{cases} \quad (4)$$

where T_{bp} is the temperature breakpoint, typically 550 °C, and T_{max} is the maximum temperature rating of the component in units of °C.

Table 2 presents the equipment cost model that follows the model proposed by [5]. The heater's cost assumes the cost correlations of the recuperators. It is an approximation since the heat source is the exhaust gases from gas turbines. New correlations are being evaluated to represent the heaters more accurately in future analyses. The equation for cooling tower, piping, and auxiliary systems costs are omitted by confidentiality.

Table 2 Summary of the scaling parameters for cost correlation. Source: Adapted from[5]

Equipment	a	SP		b
Heater	49.45	UA_{Heater}	$[W_t/K]$	0.7544
Recuperator	49.45	UA_{Recu}	$[W_t/K]$	0.7544
Cooler	32.88	UA_{Cooler}	$[W_t/K]$	0.75
Axial Turbine	182600	P_{mec}	$[MW_t]$	0.5561
Generator	108900	P_e	$[MW_e]$	0.5463
Gearbox	177200	P_{mec}	$[MW_t]$	0.2434
Compressor (centrifugal)	1230000	P_{shaft}	$[MW_t]$	0.3992
Motor	399400	P_e	$[MW_e]$	0.6062

The study adopts the net present value methodology (NPV) and Levelized Cost of Energy (LCOE) as economic evaluation criteria.

NPV is defined as:

$$NPV = \sum_{n=1}^{n=25\ years} \frac{Revenue - (Capex - Opex)}{(1 + interestrate)^n} \quad 5$$

$CAPEX$: Capital expenditure of main components.

$OPEX$: Operational expenditure including operation and maintenance.

Table 3 presents a possible distribution of the costs. CAPEX is associated with fixed capital investment (FCI), although the construction costs that make up the indirect costs were not considered in this analysis and will be implemented in the following studies.

Table 3 Total investment decomposition. Source: Adapted from [23]

Fixed capital investment (FCI)	Direct costs (DC)	Onsite costs	Purchased Equipment Costs (PEC)	Calculated
			Others	%PEC
		Offsite costs	Civil work	%PEC
			Service	%PEC
	Indirect costs (IC)	Engineering		%DC
		Construction Costs		%DC
		Contingency		%

The Levelized Cost Of Electricity (LCOE) is an aggregated indicator of the overall process costs levelized during the power plant lifetime. It encompasses annualized cost of the investment (CAPEX) using a discount rate, the operational costs, and the obtained electric production [24].

$$LCOE = \frac{CAPEX \times f_a + OPEX}{P_e \times Hour_{year}} \quad 5$$

f_a : Discount factor that considers both the risk aversion of the investor and the investment distribution over the plant lifetime.

P_e: The electrical power output of the power plant.

$Hour_{year}$: The plant availability

OPTIMIZATION STRUCTURE

This research presents the optimization analysis of the sCO_2 bottoming cycle. The analysis tool OptDesign was developed to evaluate the performance of different sCO_2 cycle architectures for various applications.

The program compiled in MATLAB® determines the thermodynamic properties (based on the Refprop® data library) for each equipment. The thermo-physical model includes knowledge of component design, component behavior, and its costs. The model is used as part of the CARBOSOLA project for thermo-economic optimization based on the equipment and the system.

Figure 4 represents the logical flow process in the OptDesign tool. Initially, the heat source in each analysis case is characterized by chemical composition, mass flow, and thermodynamic condition. Table 4 shows the input parameters that define the thermodynamic balances of the cycle. These are the decision variables in multiobjective optimization.

Table 4 Variables included in multi-objective optimization.

	Discrete variable	Range	
Pressure Level [bar]	Pressure (HP)	200 – 300	
	Pressure (LP_{Sub})	57.2 - 65.8*	
	Pressure (LP_{Sup})	75 - 110	
Heater HX1	UTTD	> 10	$UTTD = T_{21} - T_{12}$
	Effectiveness	< 0.98	$\varepsilon_{Hx_1} = \frac{T_{21} - T_{22}}{T_{21} - T_{12}}$
Recup. HTR	UTTD	> 5	$UTTD = T_2 - T_{17}$
	Effectiveness	< 0.98	$\varepsilon_{Hx_1} = \frac{T_2 - T_3}{T_2 - T_{17}}$
Split ratio	SR2	0.1 - 1	$SR_2 = \frac{\dot{m}_{16}}{\dot{m}_{14}}$
	SR3	0.1 - 1	$SR_3 = \frac{\dot{m}_{19}}{\dot{m}_{17}}$

The model initially considers the isentropic efficiency of the pump/compressor and turbine as 80% and 90%, respectively.

The computational tool performs the mass and energy balance for each equipment of the cycle through its thermophysical models. With the determined parameters, it is

possible to evaluate the turbine's isentropic efficiency for the specified operating conditions. Industrial correlations determine the efficiency of the turbine from the volumetric flow of CO2 at the equipment entrance. This similarity is not presented by confidentiality.

The calculation routines are updated with new turbine efficiency until the results reach convergence. The program counts with subroutines to investigate the heat exchangers' initial design for each evaluated condition to restrict unfeasible conditions. Once the cycle's operating conditions are determined, it performs an economic analysis to determine the equipment costs. The multi-objective optimization process means seeking a set of the best possible solutions based on a predetermined criterion. The tool allows the investigation of different objective functions, according to the analysis proposal.

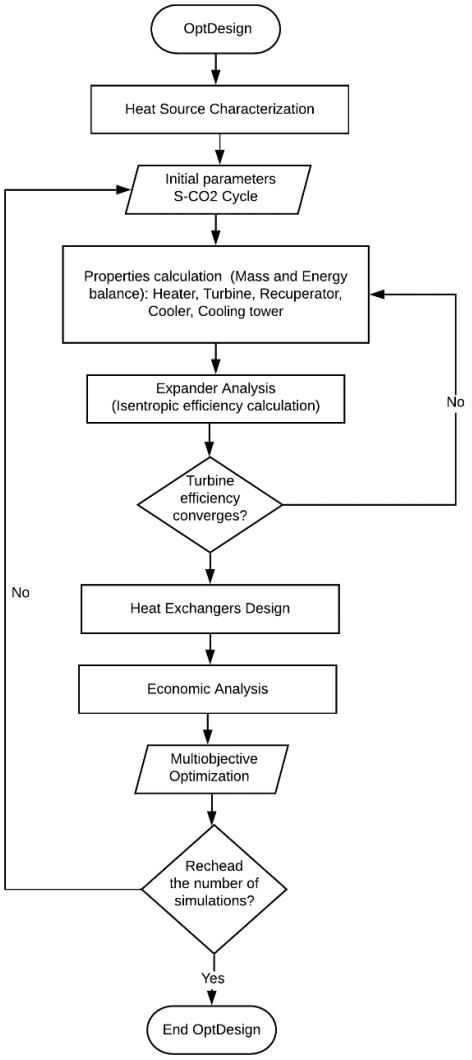

Figure 4: Flow chart of OptDesign optimization program.

The compressor inlet temperature is considered constant at 20°C. The minimum pressure of 57.29bar refers to the condensation pressure of CO_2 at 20°C, while the pressure 65.80bar determines the condensation temperature of 26°C, referring to the differential of 5K to the critical temperature of CO_2. The comparison of the results of the main components is summarized in Table 5 for an operating condition of the 3H2R cycle architecture.

A multi-objective optimization problem requires the simultaneous satisfaction of several different and generally conflicting objectives, making it impossible to find a solution that satisfies all objectives simultaneously. Therefore, it is necessary to find a set of optimal solutions. [25]

The tool performs multi-objective computer-aided optimizations for different applications and configurations of sCO_2 cycles. In this way, it allows investigating the best-operating conditions and assists in the preliminary development of the cycle's equipment and architecture.

Table 5 Validation of OptDesign Thermodynamic Model.

		Ebsilon	OptDesign	Relative error
Heater 1	[MW]	81.71	81.70	0.014%
Heater 2	[MW]	43.97	43.96	0.014%
Heater 3	[MW]	0.57	0.57	0.012%
Recuparator HTR	[MW]	63.73	63.72	0.013%
Recuparator LTR	[MW]	3.28	3.28	0.013%
Cooler	[MW]	94.40	94.39	0.013%
Turbine Power	[MW]	44.06	44.05	0.014%
Compressor Power	[MW]	12.22	12.22	0.014%
Net Power	[MW]	31.84	31.84	0.014%
Mass Flow	[kg/s]	375.80	375.75	0.013%

Each combination of the optimization variables generates a candidate vector with its responses to all the cycle characteristics. For each architectural model of the CO_2 system, initially creates a starting population for the optimization algorithms using the Design of Experiment (DOE) techniques. The DOE performs a factorial distribution of the independent variables, generating suitable initial parameters. This procedure simultaneously minimizes the quantity of data while maximizing data quality.

In this study, three optimization scenarios were investigated, having as objective functions:

- Scenario 1: Maximization of net power and minimization of Fixed Capital Investments.
- Scenario 2: Maximization of the Net Present Value and minimization of Fixed Capital Investments.
- Scenario 3: Maximization of Net Present Value and minimization of the Levelized Cost of Energy (LCOE).

RESULTS

From the multi-objective optimization process, a set of optimal solutions called the Pareto front is obtained. It allows a decision-making process to select the final solution from the optimized set. Each of Pareto's front has, on average, 2000 results, which individually gather the combination of the operating parameters of the cycle. The NPV and LCOE values are presented in a normalized format due to confidentiality.

Initially is presented the optimization solutions of the 3H2R layout for the three optimization proposals: scenarios 1, 2, and 3. This analysis will be presented to 3H2R architecture due to its complexity, extending the analysis to the maximum amount of equipment. The results obtained and the operating conditions of each cycle are strongly dependent on the analysis criteria. The effect of the analysis criteria presented is similar in the remaining architectures.

Figure 5 presents the Pareto front of optimization for scenario 1. The solutions present the direct relationship between net power and costs as expected for these types of analysis.

In this analysis, the range of higher net power comes with a more expressive increase in costs. The NPV represented by the color scale reveals that the higher net power values do not favor NPV.

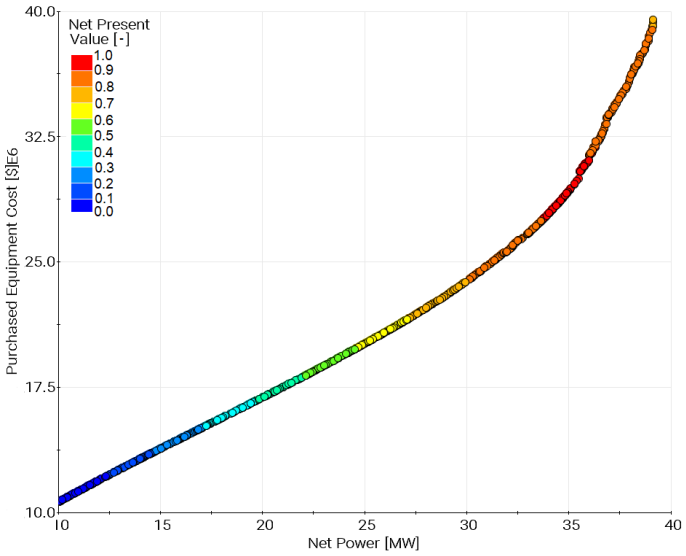

Figure 5: Results of scenario 1 of the 3H2R optimization.

Figure 6 presents the results of scenario 1 with the NPV perspective elucidating this remark.

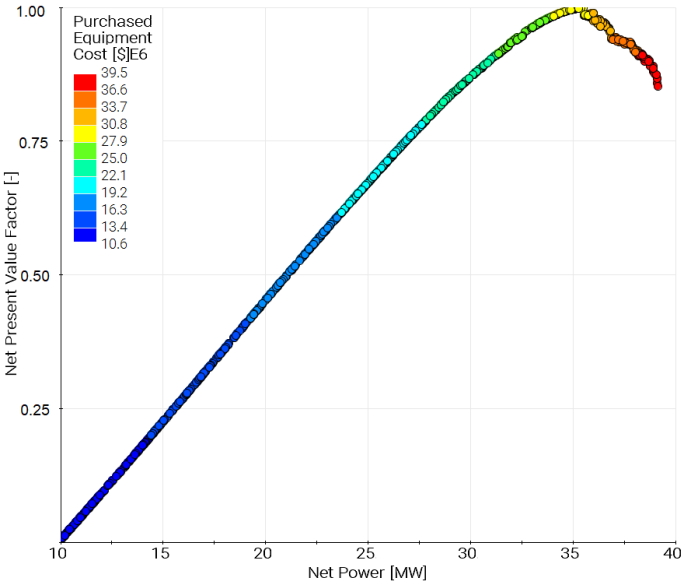

Figure 6: Scenario 1 results from an NPV perspective.

It is possible to perceive by the ascending part of the curve the limit in which the net power increase favors NPV. A sensitivity analysis on the Pareto front reveals that until reaching the NPV peak, the net power exerts a predominant factor on this parameter. While on the descending side of the curve, the costs revealed a more significant influence on it. One of the factors in this change is that higher powers are obtained with lower temperature difference in heat exchangers, significantly increasing the equipment costs.

Another relevant factor is that in the ascending range of NPV, their entirety leads to the cycle's configuration without the auxiliary expansion with the LT turbine.

The use of the LT turbine represents an additional cost of a second turbine with its auxiliary equipment. Thus, in the optimal results, the use of this equipment is justified when aiming to increase the net power, the increase of the mass flow is no longer supported by restrictions of temperature difference in heater 1.

Thus, the mass flow increase is allowed by dividing it in SR3, which is expanded in the LT turbine. These operating conditions reflect higher heat recovery in HTR and a significant increase in this equipment's costs.

The model for calculating the isentropic efficiency of the turbine is strongly dependent on the volumetric flow. The operating conditions of the CO_2 in the LT turbine penalize the equipment's efficiency, reducing to the range of 83% while the HT turbine operates close to 90%.

These factors indispose the LT turbine configuration from an NPV perspective. Although it can provide a net power increase, the LT turbine operating condition is associated with the evaluated curve's descending section.

Figure 7 presents the optimization solutions according to scenario 2. The Pareto front in this analysis is a range of the results presented in the previous analysis since the criteria that lead to NPV maximization are the same as those that lead to net power maximization. The gray representation in the graph refers to scenario 1, which here are not part of the optimal results because they provide lower NPV. This region refers to the descending part of the curve in the previous picture.

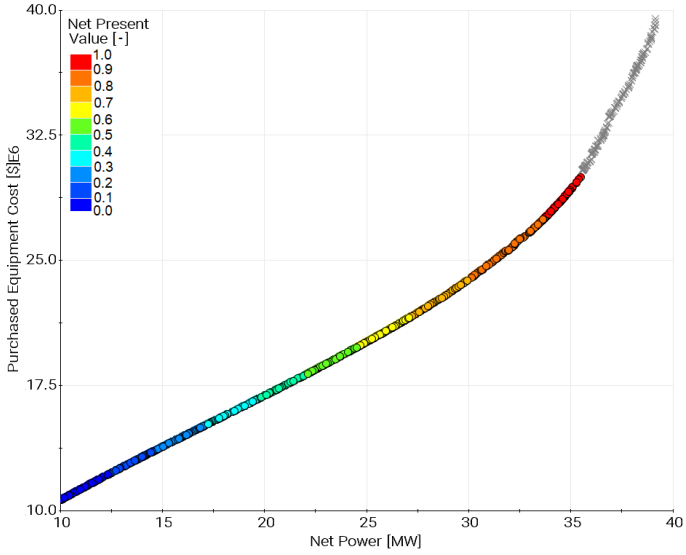

Figure 7: Results of scenario 2 of the 3H2R optimization.

The highest NPV condition, in this case, is 16.9% higher than the highest net power condition of scenario 2, even if the thermal efficiency of the cycle is 9.5% lower, and the net power is reduced in the same proportion.

Figures 8 and 9 present the cycle's exergetic analysis to maximize the net power and NPV maximization of the two optimization scenarios.

The condition that favors higher net power provides an exergetic efficiency of 67.16%, 13.7% superior to the condition in higher NPV. The net power maximization is achieved from the higher mass flow and increased heat recovery in the heat exchangers.

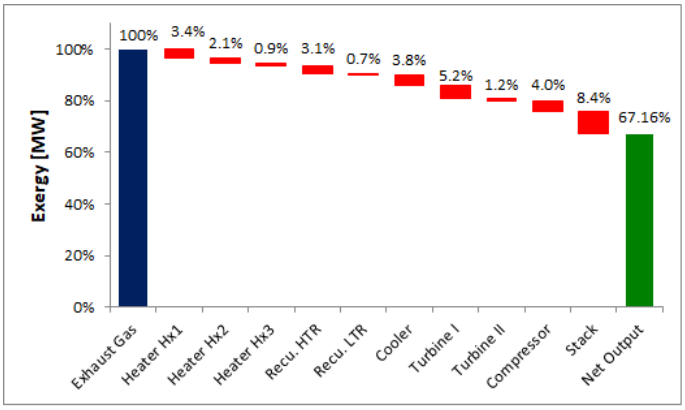

Figure 8: Exergetic analysis of higher net power condition. Optimization scenario 1.

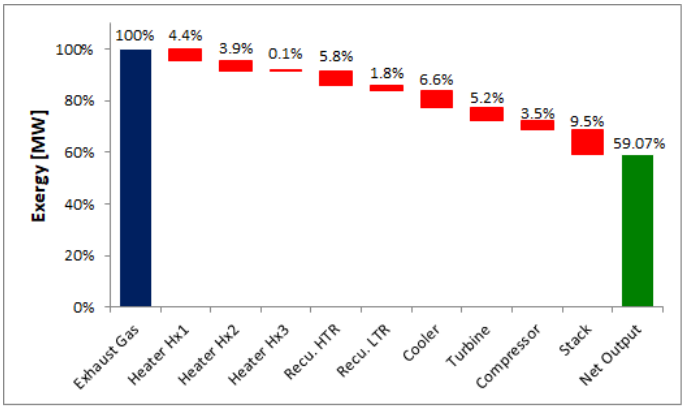

Figure 9: Exergetic analysis of higher NPV condition. Optimization scenario 2.

This analysis shows that the conditions for higher NPV operate comparatively with lower heat recovery, mainly in HTR, evidenced by the increase of exergy losses in this equipment and the cooler. There is also less heat recovery from the source, indicated by losses in heaters the stack. Although this condition leads to a less efficient cycle, it favors fewer costs by not operating with such reduced temperature differences.

Figure 10 presents the relationship between the three optimization scenarios results as reference LCOE, and net power Scenario 3 assumes LCOE minimization rather than FCI as an objective function of optimization. The color scale region represents the frontier of the optimal results of the third optimization scenario. The green band of the graph represents the optimization values of scenario 2, which are not part of the optimal solutions of the new analysis. The gray region refers to the maximization of the net power, which provides a lower NPV.

The solutions reveal that the optimal ratio from the lowest LCOE to the highest NPV corresponds to the same operating conditions of scenario 2 regarding from 84% to the maximum value of NPV. This range is associated with net powers between 31.9 and 35.5 [MW].

According to each objective function, the optimal operating ranges portion depends on the equipment's cost functions. The boundaries of the system and the costs included in the NPV and LCOE analysis are also essential to determine the cycle operation conditions.

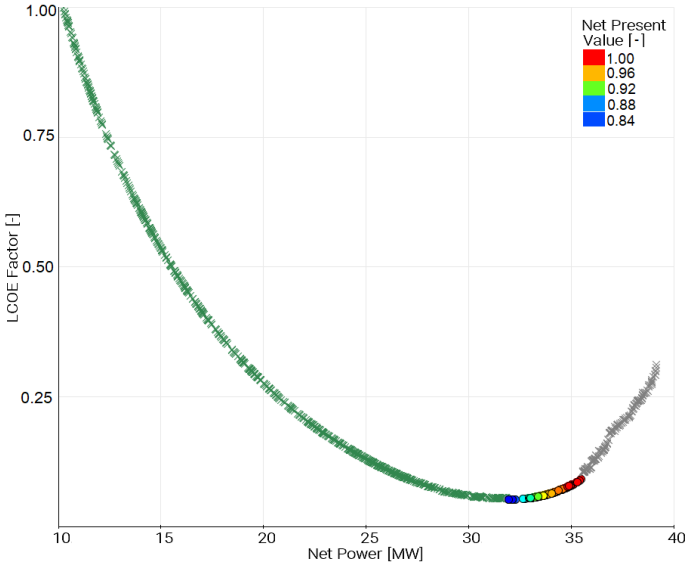

Figure 10: Scenario 3 results from a net power perspective.

ARCHITECTURE OPTIMIZATION

The three optimization approaches, scenarios 1, 2, and 3 were executed to evaluate the best operating conditions for the different sCO_2 cycle configurations: 3H2R, 2H2R, 2H1R, Regenerative, and Simple.

Optimization from the scenario 1 perspective reveals that when considering net power maximization, the more complex 3H2R and 2H2R systems allow for more efficient cycles providing higher power than the others.

Figure 11 presents each Pareto's front for scenario 2 optimization of Layouts 3H2R, 2H2R, 2H1R, Regenerative, and Simple.

The more complex 3H2R and 2H2R, although it may favor higher power ranges, which differentiate these configurations from the others, are economically penalized by the significant increase in equipment costs, not favoring NPV. In this perspective, these configurations are no longer an appreciable option.

The Regenerative and Simple layouts, less complex, are limited in their capacity to generate power. Since for the simple cycle operation, the CO_2 temperature at the turbine inlet is

significantly low (outlet temperature of the compressor), the amount of working fluid is restricted by the minimum temperature of the stack in the evaporator's mass balance. This way, the Simple cycle operates with the lower mass flow (66% of the 2H1R flow) and generates lower power.

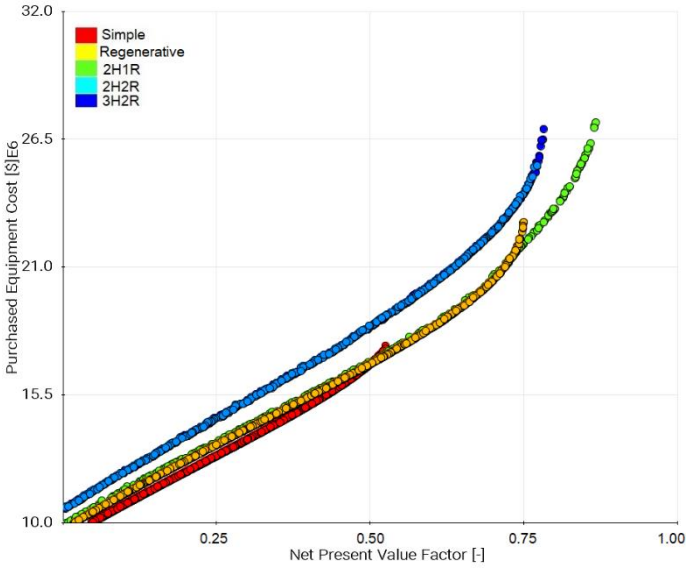

Figure 11: Optimization results of the different architectures for supercritical cycle.

The recuperator's use allows the Regenerative cycle an operation with a higher mass flow by providing a favorable condition to the working fluid at the evaporator entrance.

However, the maximum mass flow in this configuration occurs when it reaches the lower terminal temperature difference on heater 01. In this way, the heat recovered from the source in this configuration is the lowest, and the exhaust gas temperature after the heater is considerably higher.

This way, operation with the 2H1R configuration presents the best performance providing the highest NPV values associated with lower costs in subcritical and supercritical regions.

The optimization process presented in this paper also availed the subcritical operation condition. As in the supercritical operation, the 2H1R configuration had the best performance.

Figure 12 compares the optimization solutions for the 2H1R configuration to scenario 3 for supercritical and subcritical operating conditions. Comparing the optimal results in these two conditions highlights the potentialities and constraints of the supercritical cycle.

The NPV scale was normalized to the highest NPV condition, referring to the subcritical operation cycle. In this condition, the optimal solutions occur with NPV between 91.3% and its maximum value. The supercritical operation does not allow the same net power generation, and consequently, the range of optimal results corresponds to 81.5 to 88.6% of the reference value.

Analysis of the optimal solution range reveals that the net power is more significant than the costs to increase the NPV. However, this relationship is reversed in the LCOE analysis, with costs being the prominent role.

Optimal solutions occur with a small range of LCOE. This parameter has been normalized to the superior condition of the supercritical cycle. The lowest supercritical LCOE condition occurs with a 2.1% reduction, while the subcritical cycle solutions range provides 2.3 to 4.8% lower LCOE.

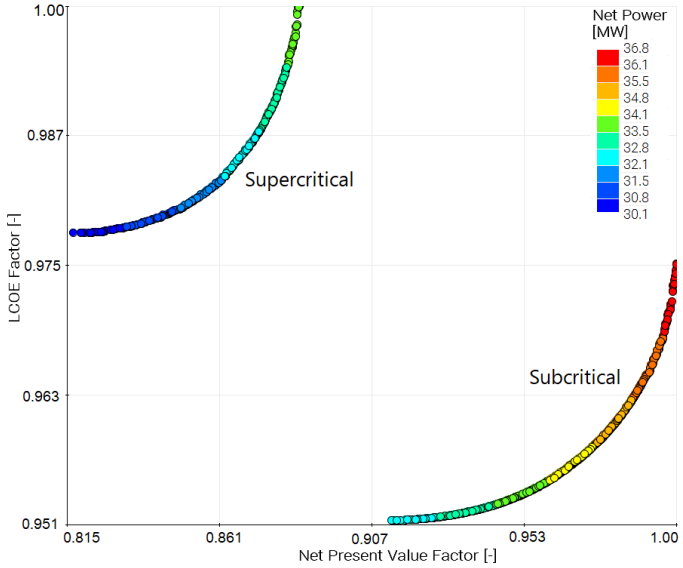

Figure 12: Comparison of 2H1R architecture optimization.

Figure 13 represents the Temperature-entropy (T-s) diagram to the maximum NPV operating parameters for both condition of 2H1R cycles.

The supercritical system is associated with lower costs, mainly related to the cooler. However, it provides less power generation in the optimum range. Since the pressure ratio in the turbine is invariably lower than in the subcritical configuration.

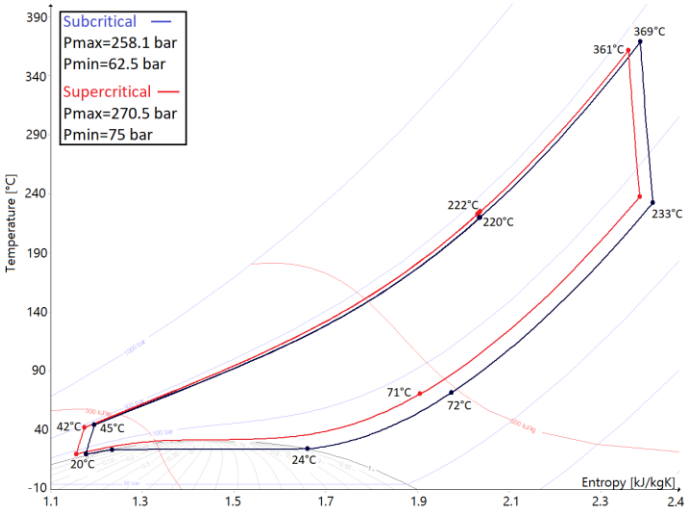

Figure 13: Operating conditions of 2H1R cycle at supercritical and subcritical conditions.

The supercritical system tends to slightly higher operating pressures and a significant increment in mass flow.

The operation with higher pressures (at turbine inlet) negatively affects the turbine's efficiency and equipment costs. Net power is a predominant aspect of this range of optimal results. Therefore, the turbine efficiency calculation is a very relevant and sensitive factor for determining the cycle's operation. As this parameter is strongly associated with CO_2 volume flow at the equipment inlet, the operating pressure range is directly related to this condition.

The turbine outlet temperature is higher in supercritical systems due to the higher pressure, limited to 75 bar. This way, it has as standard a more extensive heat recovery in the recuperator. It allows the cycle to operate with higher mass flows. These characteristics result in less heat recovery in the heater, penalizing the cycle's efficiency, to the detriment of lower equipment costs. Greater use of heat from the source would allow more significant power generation but lead to the supercritical cycle at higher costs, outside the optimal range.

Although the supercritical operation has lower costs than the subcritical, it is not enough to overcome its lower power generation power. It results in higher specific costs, higher LCOE, and a significant reduction of NPV.

Although the supercritical operation has less NPV than the subcritical cycle, it is less sensitive to variations in ambient conditions. An ambient temperature increase implies more complex restrictions in the subcritical cycle since it has lower temperature difference in the cooler.

Table 6 shows the range of each discrete variable of the optimization, referring to the range of optimal results and the analysis's immediate results. The operating conditions of heat exchangers have similar characteristics in both conditions.

Table 6 Discrete variables and main results of 2H1R optimization.

Discrete Variable		2H1R Sub.	2H1R Sup.
Pressure (HP)	[bar]	255 - 275	268 - 290
Pressure (LP)	[bar]	62.5 – 64.8	75
UTTD (Hx_1)	[-]	54 - 63	57 - 71
Effectiveness (Hx_1)	[-]	0.9 – 0.95	0.9 – 0.95
UTTD (HTR)	[-]	12 - 35	12 - 35
Effectiveness (HTR)	[-]	0.8 – 0.86	0.8 – 0.86
Results		2H1R Sub.	2H1R Sup.
Net Power	[MW]	32.2 – 36.8	30.1 – 33.9
Specific PEC	[$/kW]	772 – 823	791 - 838

The 2H1R architecture analysis reveals that the equipment contributing to the highest costs are the heaters, followed by the cooler, cooling tower, recuperator, compressor, turbine, and remaining auxiliary equipment.

Sensitivity analyses of the optimal results point out the recuperator as the decisive equipment for the cycle's optimal operation. The recuperator's operating conditions are determinant for the system's mass flow, besides managing the heater and cooler operation. This equipment plays a decisive role in determining the correct equilibrium between power and costs for the optimal operation. In this case, the cost correlations of each component are determinant for this equilibrium setting.

Optimization reveals the most profitable operation. It enables the advancement of the component cost correlation according to the equipment's design development. Further analyses with updated cost models will follow in the subsequent studies.

CONCLUSION

A thermo-economic model was performed, and three scenarios of multi-objective optimization were evaluated to determine the best conditions of five different sCO_2 cycle architecture of an exhaust/waste heat recovery cycle.

The optimization process is essential to provide the optimal operation conditions, which are very sensitive to objective functions, cost models, boundaries of the economic evaluation, equipment design, and equipment efficiency.

The 2H1R architecture configuration proposed in this study presents the most promising results. The optimal solutions for this architecture as a supercritical operation provide net power generation in the range of 30.1 - 33.9 MW and purchased equipment cost between $23.8- $28.5 million when aiming to maximize NPV and minimize LCOE.

Net power is the most relevant parameter for NPV maximization, while total costs are the main driver for LCOE analysis. Equipment cost models and economic analysis strongly influence this relation. It is decisive to the operating conditions of the cycle.

The results indicate a prominent potential for the proposed cycle configuration and operational conditions for exhaust heat recovery in a combined gas turbine sCO_2 cycle.

ACKNOWLEDGEMENTS

These investigations were conducted as part of the research project CARBOSOLA. The authors would like to thank the German Federal Ministry of Economics and Energy (BMWi) for the financial support as per resolution of the German Bundestag under grant numbers 03EE5001A (Siemens) and 03EE5001B (TU Dresden). The authors alone are responsible for the content of this paper.

NOMENCLATURE

3H2R	*3 Heaters and 2 Recuperators architecture*
2H2R	*2 Heaters and 2 Recuperators architecture*
2H1R	*2 Heaters and 1 Recuperator architecture*
CAPEX	*Capital expenditure of main C*
DC	*Direct cost*
FCI	*Fixed Capital Investment*
HT	*High temperature*
HP	*High pressure*
HTR	*High temperature recuperator*
Hx	*Heater*
IC	*Indirect cost*
LCOE	*Levelized Cost of Energy*
LMTD	*Log Mean Temperature Difference*
LP	*Low pressure*
LT	*Low temperature*
LTR	*Low temperature recuperators*
NPV	*Net Present Value*
OPEX	Operational expenditure
PEC	*Purchased Equipment Cost*
SR	*Split ratio*
VPSC	*Variable property segmented calculation*

REFERENCES

[1] Wahl A, Mertz R, Starflinger J. Experimental investigation of heat transfer in tubes to cool CO2 near the critical point in horizontal flow orientation. 18th Int. Top. Meet. Nucl. React. Therm. Hydraul. NURETH 2019, 2019, p. 2615–28.

[2] Cabeza L, Gracia A de, Fernández I, Farid M. Supercritical CO2 as heat transfer fluid: A review. Appl Therm Eng 2017;125:799–810.

[3] Xu XY, Wang QW, Li L, Chen YT, Ma T. Study on thermal resistance distribution and local heat transfer enhancement method for SCO2-water heat exchange process near pseudo-critical temperature. Int J Heat Mass Transf 2015;82:179–88.

[4] Xiao G, Xing K, Zhang J, Yang T, Ni M, Cen K. Heat Transfer Characteristics of Sco2 and Dynamic Simulation Model of Sco2 Loop. 3 Rd Eur Supercrit CO2 Conf 2019:1–11..

[5] Weiland NT, Lance BW, Pidaparti S. SCO2 POWER CYCLE COMPONENT COST CORRELATIONS FROM DOE DATA SPANNING MULTIPLE SCALES AND APPLICATIONS 2019:1–17.

[6] Wright SA, Davidson CS, Scammell WO. Thermo-Economic Analysis of Four sCO2 Waste Heat Recovery Power Systems. 5th Int Symp - Supercrit CO2 Power Cycles 2016:1–16.

[7] Carlson MD, Middleton BM, Ho CK. Cycles Using Component Cost Models Baselined With Vendor Data. Proc ASME 2017 Power Energy Conf 2017:1–7.

[8] Penkuhn M, Tsatsaronis G. Thermoeconomic modeling and analysis of sCO2 Brayton cycles 2019.

[9] Milani D, Luu MT, McNaughton R, Abbas A. Optimizing an advanced hybrid of solar-assisted supercritical CO2Brayton cycle: A vital transition for low-carbon power generation industry. Energy Convers Manag 2017;148:1317–31. https://doi.org/10.1016/j.enconman.2017.06.017.

[10] Crespi F, Gavagnin G, Sánchez D, Martínez GS. Analysis of the Thermodynamic Potential of Supercritical Carbon Dioxide Cycles: A Systematic Approach. J Eng Gas Turbines Power 2018;140:1–10..

[11] Wang K, He YL, Zhu HH. Integration between supercritical CO2 Brayton cycles and molten salt solar power towers: A review and a comprehensive comparison of different cycle layouts. Appl Energy 2017;195:819–36.

[12] Wang K, Li MJ, Guo JQ, Li P, Liu Z Bin. A systematic comparison of different S-CO2Brayton cycle layouts based on multi-objective optimization for applications in solar power tower plants. Appl Energy 2018;212:109–21.

[13] Liao G, Liu L, E J, Zhang F, Chen J, Deng Y, et al. Effects of technical progress on performance and application of supercritical carbon dioxide power cycle: A review. Energy Convers Manag 2019;199:23.

[14] Held TJ. Supercritical CO2 cycles for gas turbine combined cycle power plants. Power Gen Int 2015.

[15] Mecheri M, Zhao Q. Probabilistic technique for solving computational problem: application of ant colony optimization (aco) to find the best sco2 brayton cycle configuration. 3nd Eur Supercrit CO2 Conf Sept 19-20, 2019, Paris, Fr 2019:1–14.

[16] Giegel J. Heat Engine System Having a Selectively Configurable Working Fluid Circuit. 20150076831, 2015.

[17] Glos S, Wechsung M, Wagner R, Heidenhof A, Schlehuber D. Evaluation of sCO2 power cycles for direct and waste heat applications. 2nd Eur Supercrit CO2 Conf 2018:0–10.

[18] Wagner R. Thermodynamische Analyse von Sperrvermerk Verbleib der Exemplare 2018.

[19] Johnson G a, Mcdowell MW, Connor GMO, Sonwane CG. Supercritical CO2 Cycle Development at Pratt and Whitney Rocketdyne. ASME Turbo Expo 2012 2012.

[20] Kimzey G. Development of a Brayton Bottoming Cycle using Supercritical Carbon Dioxide as the Working Fluid. EPRI Rep 2012:1–31.

[21] Cho SK, Kim M, Baik S, Ahn Y, Lee JI. Investigation of the bottoming cycle for high efficiency combined cycle gas turbine system with supercritical carbon dioxide power cycle. Proc ASME Turbo Expo 2015;9:1–12.

[22] Ke H, Xiao Q, Cao Y, Ma T, Lin Y, Zeng M, et al. Simulation of the printed circuit heat exchanger for S-CO2 by segmented methods. Energy Procedia 2017;142:4098–103..

[23] Canepa R, Zunino P. Combined cycle power plant thermo-economic multi-objective optimization using evolutionary algorithm. 2014:1–10.

[24] Zhao Q. Conception and optimization of supercritical CO2 Brayton cycles for coal-fired power 2019.

[25] Sotomonte C, Gotelip T, Coronado C., Nascimento M. Multi-objective optimization for a small biomass cooling and power cogeneration system using binary mixtures. Appl Therm Eng 2021;182.

ANNEX A

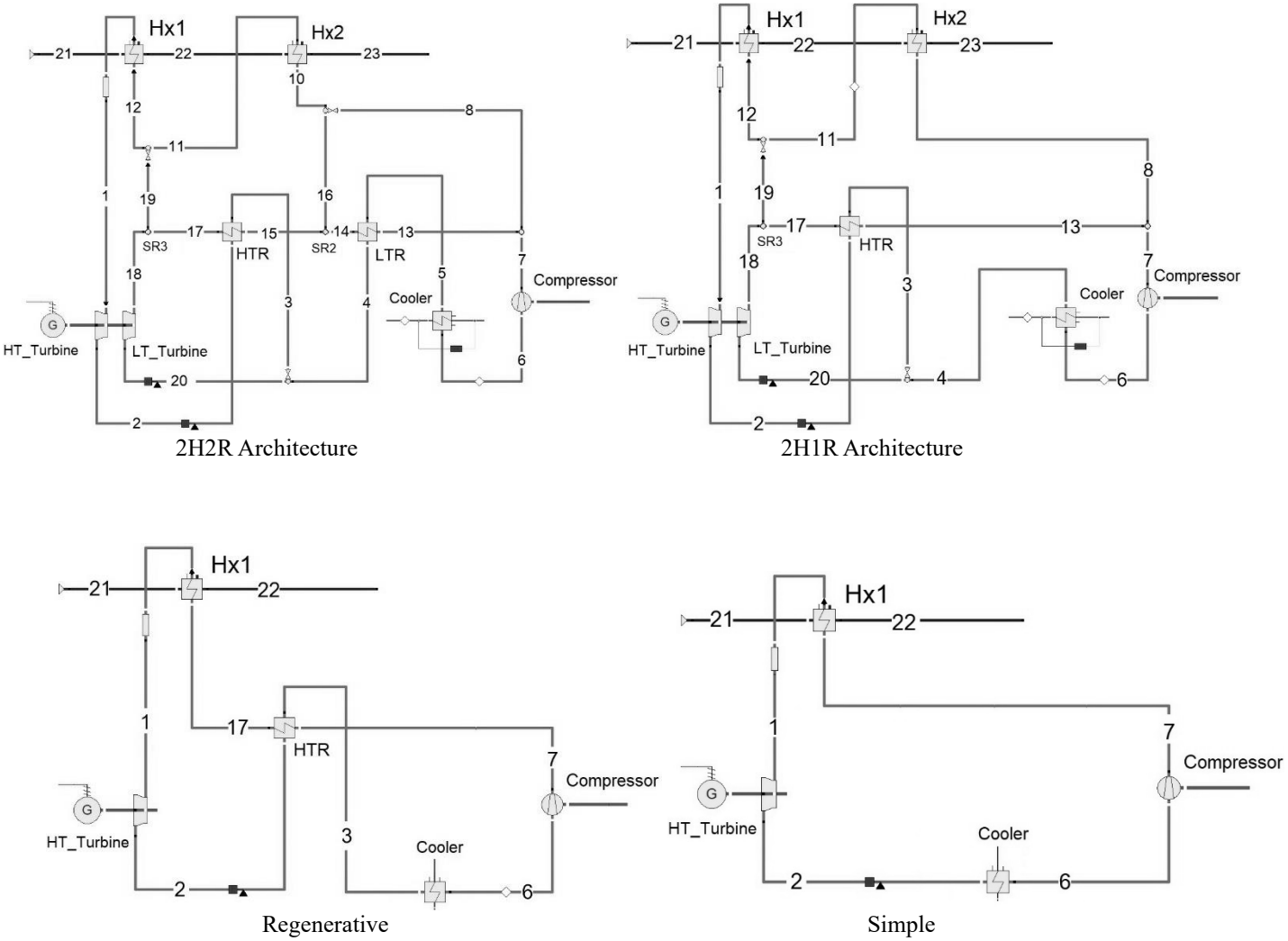

Figure 14: Classification of evaluated sCO_2 architectures.